

Electrongun

1 Overview

- all computations use the full beamtube (1.5 m)
- plots of the electrostatic potential and electric field exist as well as convergence studies
- still need to rerun the convergence study as implemented for the photocathode

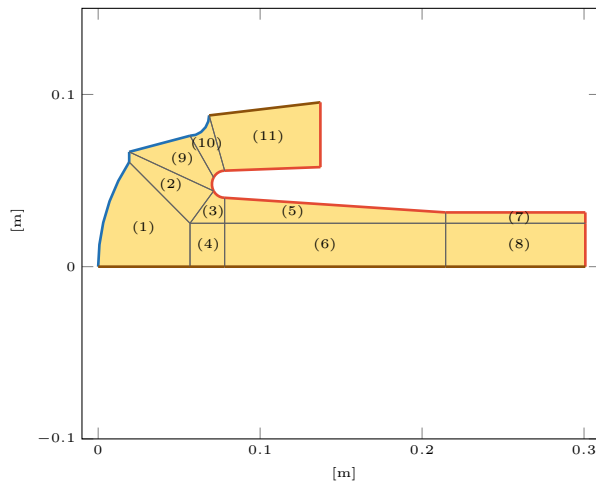


Figure 1: shortened geometry including patches and boundary conditions

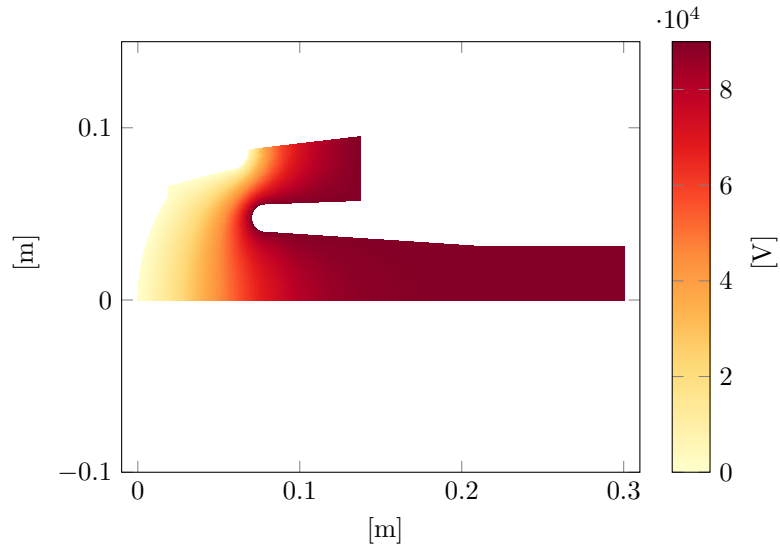


Figure 2: electrostatic potential with degree $p = 2$ and $n_{\text{sub}} = 8$

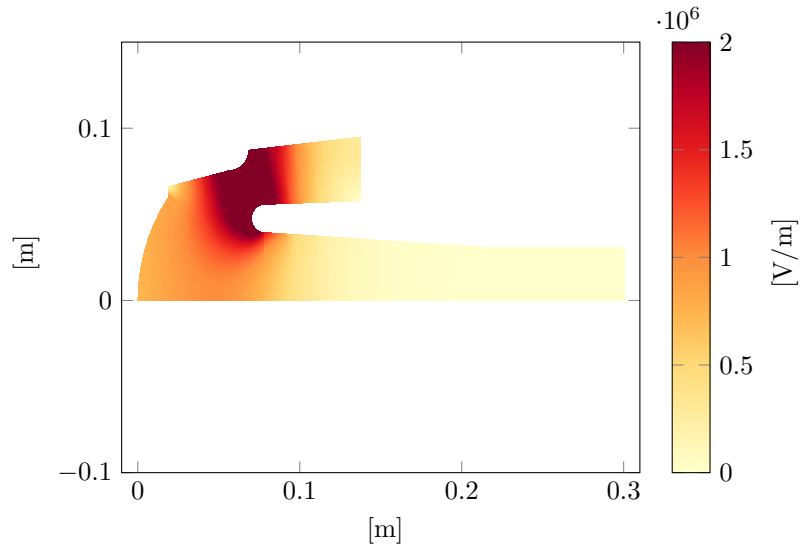


Figure 3: absolute value of electric field with $p = 2$ and $n_{\text{sub}} = 8$

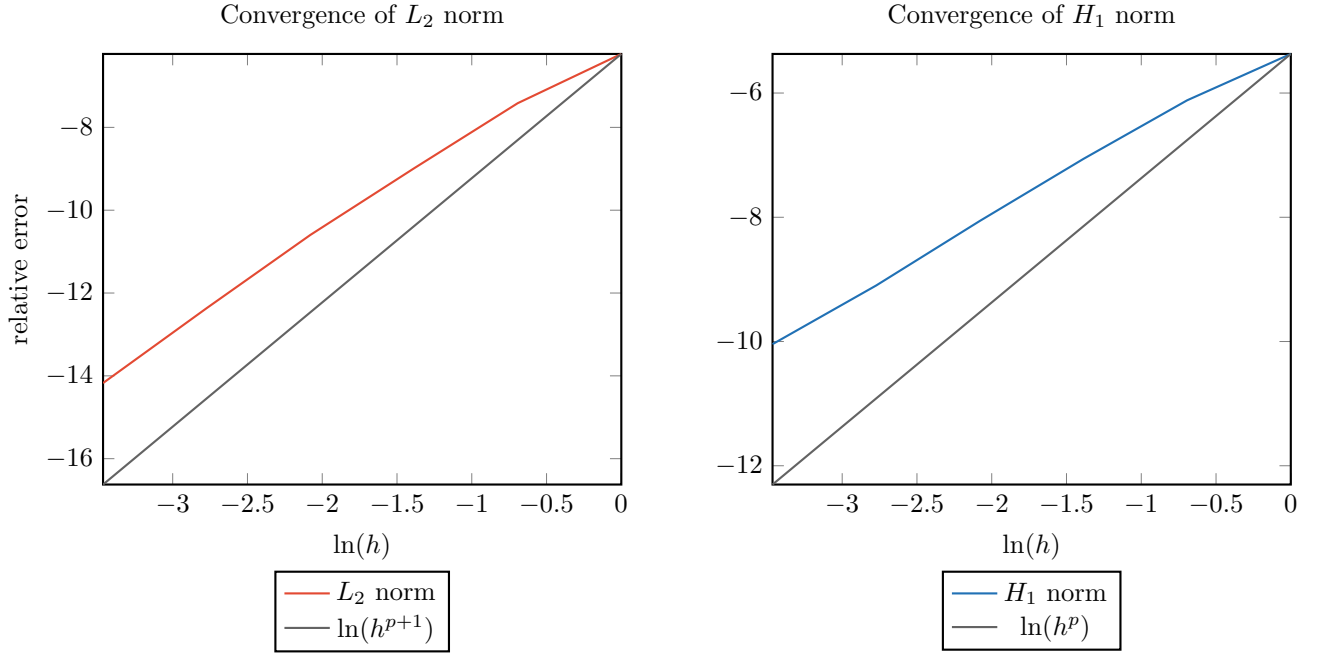


Figure 4: reference uses $p = 3$ and $n_{\text{sub}} = 64$, relative error uses maximum potential/field value, deprecated version

2 Tracking

- integrator uses different number of steps in each simulation (due to adaptivity), thus only approximation of error possible

The convergence study for the fieldmap is based on the size of the hexahedra used by ASTRA for the interpolation. h is chosen as the main diagonal of the cuboids. The study is performed for different starting points of the probe particle, centeraxis indicates the starting position $(0, 0, 0)$, offaxis stands for $(0.3, 0.7, 0)$ and onaxis represents $(0, 0.5, 0)$ where all the coordinates are chosen in the parametric domain. Furthermore a second study with another IGA solution after knot refinement was performed.

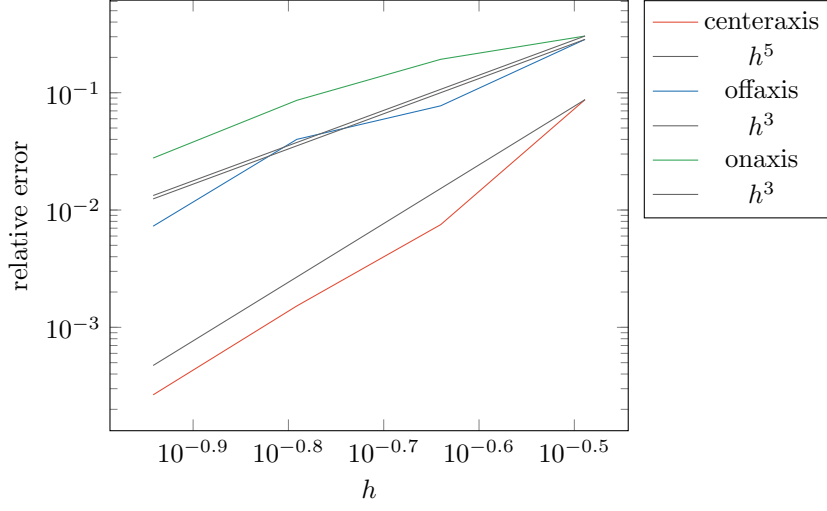


Figure 5: convergence of fieldmap with $n_{\text{sub}} = 8$

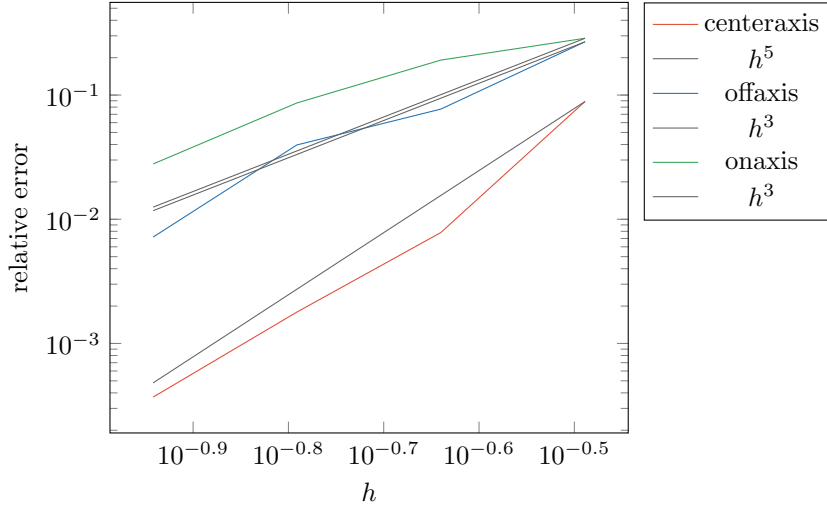


Figure 6: convergence of fieldmap with $n_{\text{sub}} = 32$

The results in fig. 5 and fig. 6 show similar convergence behavior for either IGA solution. Furthermore the convergence rate appears much lower for off center probe particles although there is no large difference between different off center starting points.

The convergence study for the time integrator was again performed for the different starting points and also for field maps based on grids of varying size.

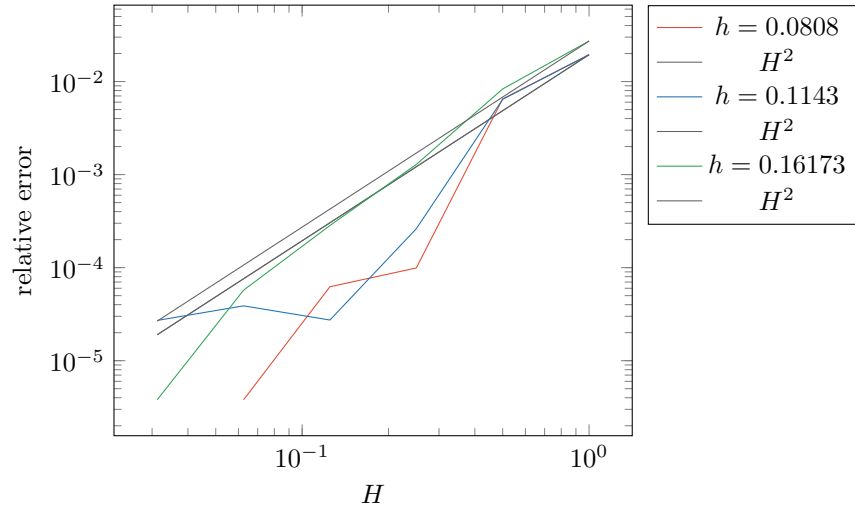


Figure 7: convergence of time integrator for centeraxis case

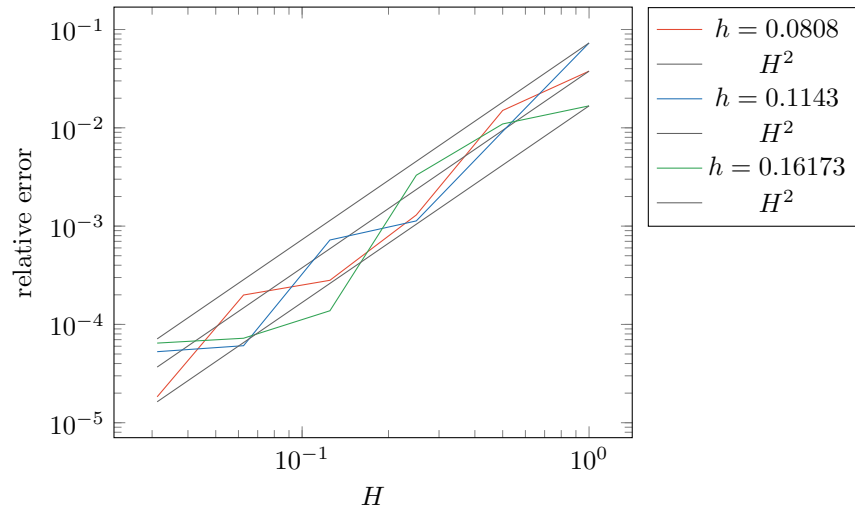


Figure 8: convergence of time intergrator for onaxis case

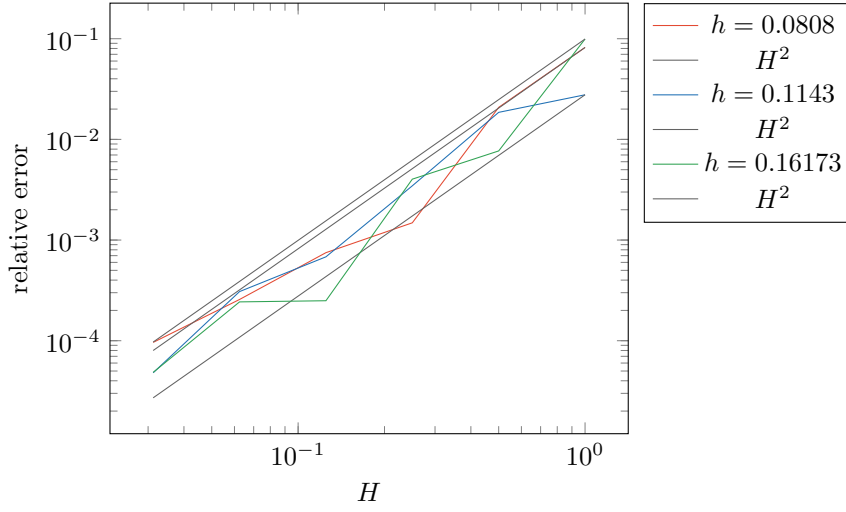


Figure 9: convergence of time integrator for offaxis case

The results in fig. 7, fig. 8 and fig. 7 show similar results compared with the grid convergence study. For the probe particle starting on the center axis the convergence rate appears to be higher then in the other cases, however the rates seem to be independent from the fieldmap for off center axis particles.

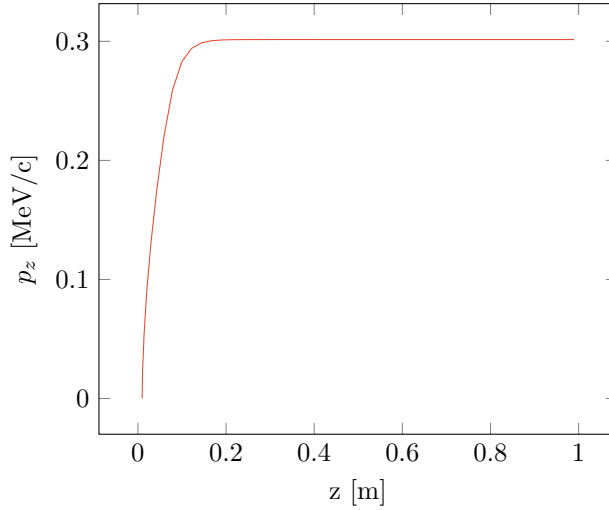


Figure 10: longitudinal momentum of probe particle during simulation

Fig. 10 shows the longitudinal momentum component of an on axis particle during simulation.

- emission is handled on my side, either uniformly or normally distributed particles

- both types depend on multiple parameters: total charge Q , number of particles N_{prt} , number of probe particles
- emission is performed based on the rotated 2D cathode

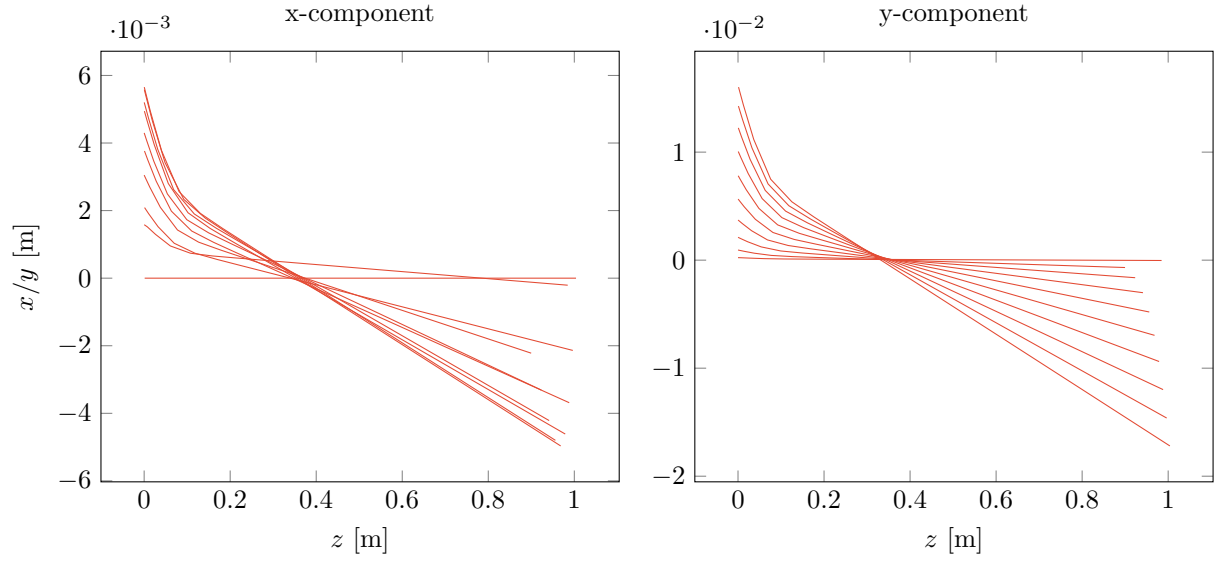


Figure 11: trajectories of probe particles for normal distribution without space charge

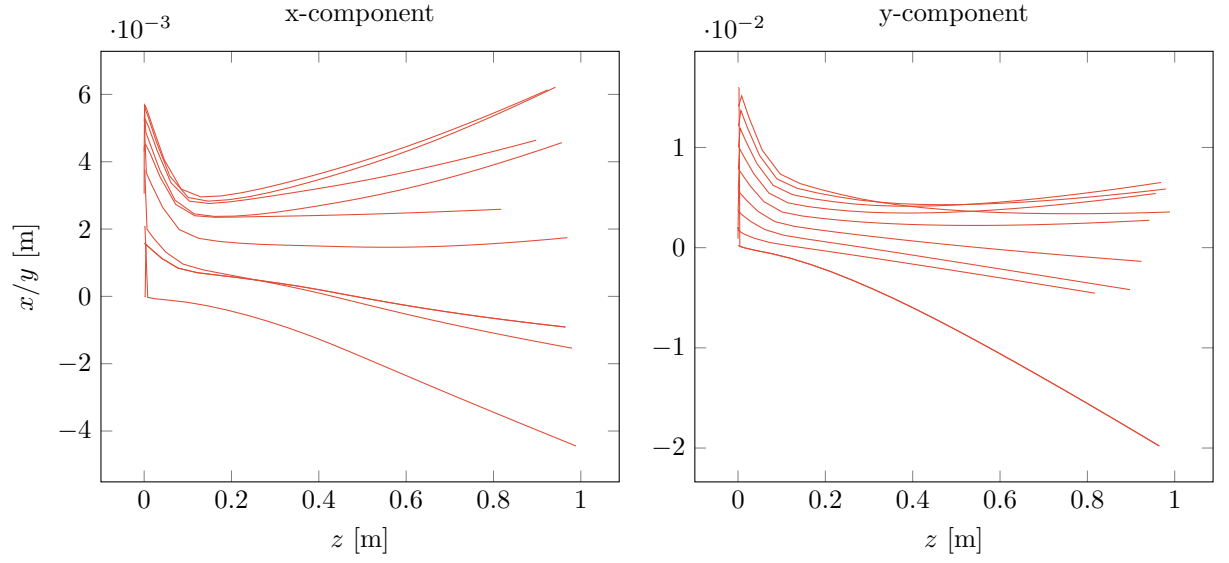


Figure 12: trajectories of probe particles for normal distribution with space charge

Fig. 11 and fig. 12 show the tracking results for 10 probe particles with a total number of 100 normally distributed particles once without and once with space charge effects included. The inclusion of space charge leads to vastly different behavior. It should be noted that there appears to be a bug in the indexing scheme of the output files, since the particle trajectories seem to jump during the first few steps.

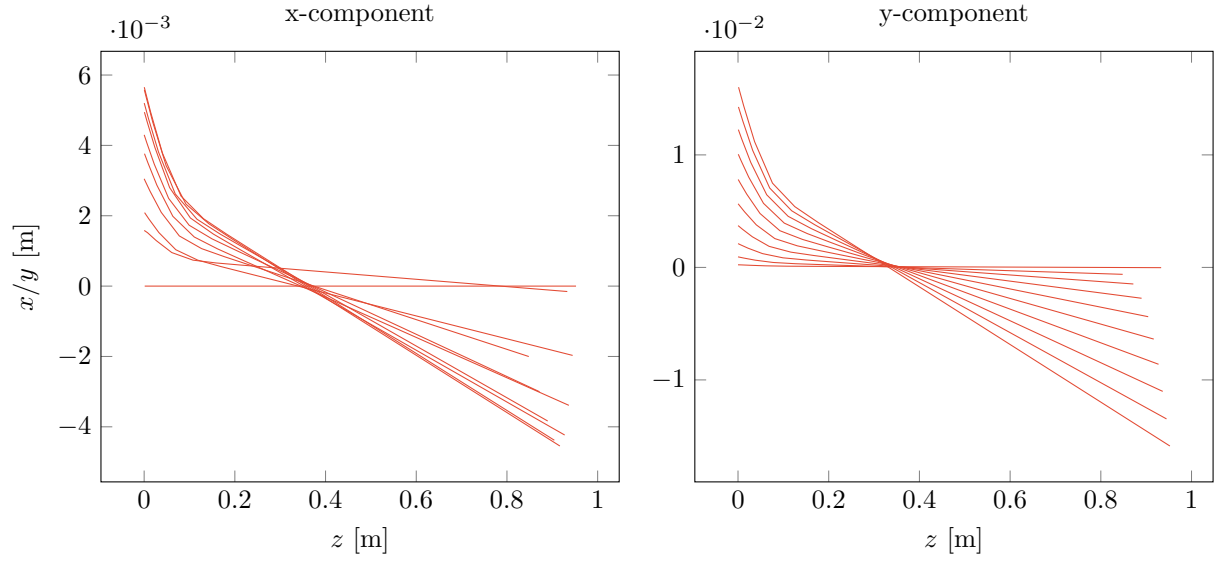


Figure 13: trajectories of probe particles for uniform distribution without space charge

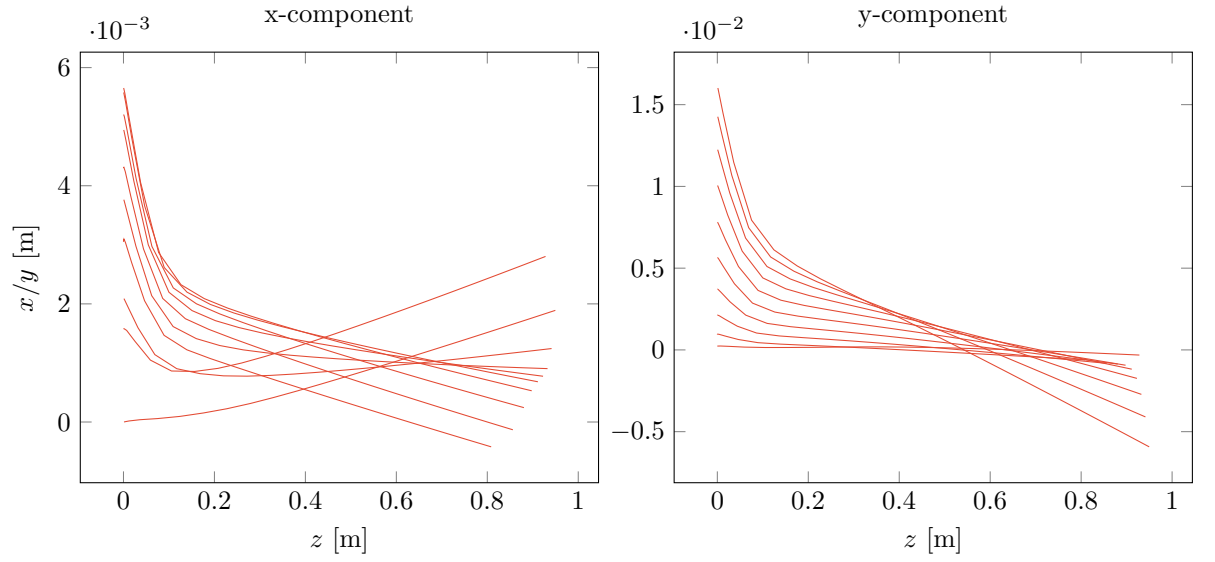


Figure 14: trajectories of probe particles for uniform distribution with space charge

Fig. 13 and fig. 14 show the tracking results for 10 probe particles with a total number of 100 uniformly distributed particles once without and once with space charge effects included. The inclusion of space charge again leads to different behavior, however the differences are not as large as before.

3 Optimization

- cost function uses outermost beam minimum, distance of beam minima and radial derivatives of minima
- extra constraint to force continuity at $(0,0)$
- start with straight cathode
- only load the geometry once and manipulate control points (increase number of control points with each optimization cycle)